

ATPase and Shortening Rates in Frog Fast Skeletal Myofibrils by Time-Resolved Measurements of Protein-Bound and Free P_i

Tom Barman,* Martin Brune,# Corinne Lionne,* Nicoletta Piroddi,§ Corrado Poggesi,§ Robert Stehle,* Chiara Tesi,§ Franck Travers,* and Martin R. Webb#

*INSERM U128, IFR 24, 34293 Montpellier, France; §Dipartimento di Scienze Fisiologiche, Università degli Studi, I-50134 Firenze, Italy; and #National Institute for Medical Research, Mill Hill, London NW7 1AA, United Kingdom

ABSTRACT Shortening and ATPase rates were measured in Ca^{2+} -activated myofibrils from frog fast muscles in unloaded conditions at 4°C. ATPase rates were determined using the phosphate-binding protein method (free phosphate) and quench flow (total phosphate). Shortening rates at near zero load (V_o) were estimated by quenching reaction mixtures 50 ms to 10 s old at pH 3.5 and measuring sarcomere lengths under the optical microscope. As with the rabbit psoas myofibrils (C. Lionne, F. Travers, and T. Barman, 1996, *Biophys. J.* 70:887–895), the ATPase progress curves had three phases: a transient P_i burst, a fast linear phase (k^F), and a deceleration to a slow phase (k^S). Evidence is given that k^F is the ATPase rate of shortening myofibrils. V_o is in good agreement with mechanical measurements in myofibrils and fibers. Under the same conditions and at saturation in ATP, V_o and k^F are 2.4 μm half-sarcomere $^{-1}$ s $^{-1}$ and 4.6 s $^{-1}$, and their K_m values are 33 and 200 μM , respectively. These parameters are higher than found with rabbit psoas myofibrils. The myofibrillar k^F is higher than the fiber ATPase rates obtained previously in frog fast muscles but considerably lower than obtained in skinned fibers by the phosphate-binding protein method (Z. H. He, R. K. Chillingworth, M. Brune, J. E. T. Corrie, D. R. Trentham, M. R. Webb, and M. R. Ferenczi, 1997, *J. Physiol.* 50:125–148). We show that, with frog as with rabbit myofibrillar ATPase, phosphate release is the rate-limiting step.

INTRODUCTION

A central problem in muscle contraction is to relate the mechanical events to the ATPase activity of the myosin heads. Historically, the bulk of muscle mechanics was carried out with fast muscle fibers from frog (Gordon et al., 1966; Ford et al., 1977; Huxley, 1980) whereas the ATPase experiments were almost exclusively confined to actomyosin from rabbit skeletal muscle (Trentham et al., 1976; Taylor, 1979; Geeves, 1991). Ideally, one should obtain the mechanical and chemical kinetic data on the same system, under identical conditions and simultaneously. This was the aim of Hill (1938) who approached the problem of the energy transduction in muscle by studying enthalpy production (heat plus work) in different conditions of contraction. A number of energy balance studies have been carried out to attempt to correlate enthalpy production with chemical energy input, i.e., with the rate of ATP breakdown (reviewed in Kushmerick, 1983, and Woledge et al., 1985). However, in these studies, which were carried out on whole frog muscle preparations, it was not possible to separate the components of the energy transduction mechanism, especially those involving the connection between the mechan-

ical steps and the kinetics of the ATPase of the myosin heads.

In Lionne et al. (1996), we suggested that, by the use of myofibrils, one can study simultaneously the biochemical and mechanical properties of muscle contraction. Myofibrils are the functional contractile units of muscle, and yet they are small enough for study by rapid transient kinetic methods. They appear to be fully regulated and, unlike actomyosin, can be activated at physiological ionic strengths. With myofibrils, chemical kinetic (Ma and Taylor, 1994; Lionne et al., 1996; Chaen et al., 1997, and references cited therein) and mechanical (Bartoo et al., 1993; Friedman and Goldman, 1996; Colomo et al., 1997) studies have been carried out.

In Lionne et al. (1996), we tried to measure simultaneously the shortening and ATPase rates of rabbit psoas myofibrils. The attempt was based on the shape of the ATPase progress curves obtained with shortening myofibrils. These are characterized by three phases: an initial P_i burst, an apparently linear phase (fast steady-state rate, k^F), and then a deceleration to a slow linear phase (slow steady-state rate, k^S). We proposed that k^F is the ATPase of myofibrils that are shortening rapidly under zero external load and k^S the ATPase rate of overcontracted myofibrils.

Here we studied the ATPases of frog myofibrils with four objectives. First, as the experiments with rabbit psoas myofibrils were carried out at the unphysiologically low temperature of 4°C, it was important to extend the study to myofibrils from a cold-blooded animal. Second, the rabbit myofibrillar ATPase profile was compared with that of a muscle preparation having different mechanical properties. The slack sarcomere length of frog fibers is shorter than in

Received for publication 30 December 1997 and in final form 11 March 1998.

Dr. Stehle's present address: Institut für Vegetative Physiologie der Universität Köln, Robert-Koch Strasse 39, D-50931 Köln, Germany.

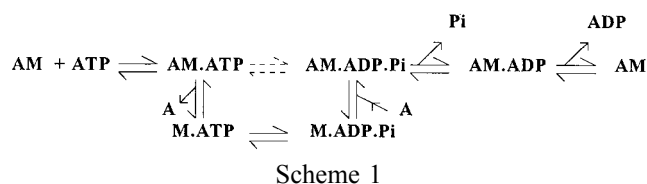
Address reprint requests to Dr. C. Poggesi, Dipartimento di Scienze Fisiologiche, Università degli Studi, Viale G.B. Morgagni 63, I-50134 Firenze, Italy. Tel: 39-55-423-7341; Fax: 39-55-437-9506; E-mail: poggesi@cesit1.unifi.it.

© 1998 by the Biophysical Society

0006-3495/98/06/3120/11 \$2.00

rabbit fibers (2.0 μm versus 2.3–2.6 μm). Furthermore, the maximal shortening velocity, V_0 , of frog fibers is faster than that of rabbit fibers. Thus, at 2–5°C, V_0 values of 2.4–2.7 ($\mu\text{m}/\text{half-sarcomere (h.s.)s}^{-1}$) were reported for frog fibers (Cecchi et al., 1978; Edman, 1979; Ferenczi et al., 1984) compared with 0.6–0.8 ($\mu\text{m}/\text{h.s.})\text{s}^{-1}$ for rabbit psoas fibers (Brenner, 1980; Ford et al., 1991; Pate et al., 1994). Third, the ATPase rate was determined for rapidly shortening myofibrils isolated from frog myofibrils. Is the higher V_0 of fast frog skeletal muscles compared with rabbit psoas muscle accompanied by a higher k^F ? Finally, the use of myofibrils provides a more stable system than has been available hitherto (Ferenczi et al., 1978a,b).

We studied the ATPases of myofibrils from frog fast muscles by two methods: the phosphate-binding protein (PBP) method of Brune et al. (1994) (in which free P_i is measured specifically) and the quench-flow technique (in which reaction mixtures are quenched in acid and total P_i is determined). We interpret our results by Scheme 1:



where M represents myosin heads and A actin (thin filament).

In the presence of Ca^{2+} , the ATPase progress curves with frog and rabbit myofibrils are qualitatively similar: an initial P_i burst, a fast ATPase rate, and then a deceleration to a slow ATPase. However, there are significant quantitative differences: the fast ATPase rate is considerably faster and the K_m for ATP larger with frog than with rabbit myofibrils. Myofibrillar shortening rates by quench flow are in good agreement with those obtained from mechanical studies on fibers and myofibrils. Finally, we present evidence that, with frog as with rabbit myofibrillar ATPase (Lionne et al., 1995), P_i release is the rate-limiting step.

MATERIALS AND METHODS

Myofibrils

Myofibrils were prepared from fast skeletal muscle (tibialis, sartorius, or mixed fast hindlimb muscles) of the frog (*Rana ridibunda*) as in Colomo et al. (1997). To provide myofibrils of sarcomere lengths of 2.25 μm , the muscle fibers had been stretched (Knight and Trinick, 1982; Lionne et al., 1996). Myofibrillar ATPase and shortening velocities are easier to study when their sarcomere lengths are 2.25 μm rather than the 2.0 μm obtained without stretching. At 2.25 μm , the overlap is 100% (Huxley, 1980).

Before use, the myofibrils were washed in the experimental buffer (2 \times 10 vol) and filtered through a polypropylene filter of 149- μm pore size (Spektrum, Houston, TX). The preparations were kept on ice and used within 3 h.

Phosphate-binding protein

The free P_i probe was the A197C mutant of the *Escherichia coli* PBP that had been labeled specifically at the introduced cysteine with the fluoro-

phore *N*-[2-(1-maleimidyl)ethyl]-7-diethylamino coumarin-3-carboximide (MDCC) (Brune et al., 1994).

Measurement of myosin head concentrations

The total protein concentration in the myofibrils was determined by dissolving the myofibrils in 2% SDS, 0.1 M NaCl, and 50 mM Tris, pH 7.4, and measuring the absorbance at 280 nm. The extinction coefficient was determined as in Herrmann et al. (1993) with rabbit skeletal muscle myosin and actin as reference proteins and gave $E_{1\%}^{280} = 7$. The proportion of myosin in the myofibrils was determined from SDS-polyacrylamide gel electrophoresis stained with Coomassie blue and, as for rabbit psoas myofibrils, was 50% of the total protein. The molar concentration of myosin heads in the preparations was calculated assuming that the molecular weights of rabbit and frog skeletal myosins are identical (Ferenczi et al., 1978a).

ATPase measurements by quench flow (acid quench: total P_i)

Quench-flow ATPase measurements were carried out in home-built thermostatically controlled quench-flow apparatuses (Barman and Travers, 1985). The procedure was to mix myofibrils with [γ - ^{32}P]ATP in an apparatus, allowing the mixture to age, quenching it in acid (22% trichloroacetic acid plus 1 mM KH_2PO_4), and then determining the [^{32}P] P_i by the filter paper method of Reimann and Umfleet (1978). The P_i determined is the sum of free and enzyme-bound P_i (see Scheme 1). The concentrations of the reagents used are given in the legends to the figures.

ATPase measurements by fluorescence stopped flow (MDCC-PBP: free P_i)

Fluorescence stopped-flow ATPase measurements were carried out in a Hi-Tech Scientific (Salisbury, UK) fluorescence stopped-flow apparatus (model SF-61 DX2). Typically, both syringes of the apparatus contained 10 μM MDCC-PBP. A P_i mop system (0.1 U/ml purine nucleoside phosphorylase plus 0.3 mM 7-methylguanosine) was added to both syringes to ensure removal of trace amounts of P_i . The excitation and emission wavelengths were 436 nm and >455 nm, respectively. For full details of the procedures used, including precaution (P_i contamination), see Brune et al. (1994) and Lionne et al. (1995). By this method, one determines free P_i only (Scheme 1).

Myofibrillar shortening velocity measurements

Myofibrillar shortening experiments were carried out by the quench-flow method. Shortening was initiated by the addition of ATP to Ca^{2+} -activated myofibrils and stopped by quenching in 0.2 M potassium formate, pH 3.5. The results of control experiments revealed that the pH 3.5 quench was rapid and that it did not affect the myofibrillar structures, in particular, the sarcomere lengths (as seen under the microscope). Merely passing the myofibrils through the quench-flow apparatus (without the addition of ATP or quencher) did not appear to affect the structures either.

Sarcomere lengths were measured using a Leica DMR microscope equipped with bright-field optics. Images were collected by a Hamamatsu C5985 CDD camera (Hamamatsu, Japan), stored on a computer, and displayed on a high-resolution monitor. The total magnification was $\times 2000$. Measurements were made using a grid placed on the screen of the monitor that had been calibrated with a Nikon micrometer slide. For each time point, sarcomere lengths were measured in 20–40 different myofibrils. The average sarcomere length in each of these myofibrils was obtained by measuring the lengths of straight portions (with at least five sarcomeres) and then dividing this by the number of sarcomeres in the portions.

Experimental conditions and chemicals

The basic buffer was 0.1 M potassium acetate, 5 mM KCl, and 50 mM Tris adjusted to pH 7.4 with acetic acid. Under relaxing conditions, the buffer contained 2 mM EGTA and 5 mM magnesium acetate. Under activating conditions, it contained 0.1 mM CaCl_2 and 2 mM magnesium acetate. The sources of the chemicals are given in Herrmann et al. (1993) and Lionne et al. (1996).

RESULTS

Overall ATPases of frog fast muscle myofibrils

Quench-flow experiments

Typical time courses for ATP hydrolysis by tibialis myofibrils at 60 μM ATP and 4°C under relaxing and activating conditions are shown in Fig. 1.

Under relaxing conditions, the time course consisted of a rapid burst of P_i , a short linear phase (possibly a manifestation of transient rigor activation), and then a slow steady-

state rate of 0.04 s^{-1} . Direct microscope observation of reaction mixtures at different times (i.e., without the acid quench) showed that, under relaxing conditions, the myofibrils did not shorten.

Under activating conditions, the time course for ATP hydrolysis consisted of three phases. As a first approximation, we interpret these as we did for the rabbit psoas myofibrils (Lionne et al., 1996): an initial rapid P_i burst phase (confirmed below) and a rapid apparently linear phase (rate constant k^F , 3.2 s^{-1}) followed by a slow linear phase (k^S , 0.9 s^{-1}).

At 60 μM ATP, Ca^{2+} -activated the ATPase ~ 70 -fold. This suggests that the myofibrils have the complete regulatory apparatus of the muscle. Myofibrils from the frog sartorius muscle and mixed fast hindlimb muscles gave very similar time courses (results not illustrated).

We then attempted to determine the ATP dependences of the myofibrillar parameters, in particular, to obtain saturation in their kinetics. This was not easy because, to attain saturation kinetics with frog myofibrils, high ATP and therefore high myofibrillar concentrations are needed, which are difficult to handle in our quench-flow apparatus. The myofibrillar ATPase experiments were continued using the PBP method of Brune et al. (1994) in a stopped-flow apparatus.

Stopped-flow experiments

The procedure of Brune et al. (1994) has the following advantages over the quench-flow method. First, higher ATP concentrations can be used. Second, it is a continuous method, so theoretically it is a more accurate way of testing for linearity of P_i production than the point-by-point quench-flow method. Third, it is specific for free P_i and so allows one to determine the nature of the transient P_i burst phase in the quench-flow experiments. Fourth, as lower myosin head concentrations can be used, less ATP is used per turnover so it suffers less from ATP depletion (K_M effect, inhibition by ADP).

A typical time course for free P_i production with Ca^{2+} -activated tibialis myofibrils at 60 μM ATP is shown in Fig. 1 *B*. The overall shape of the course is very similar to that by the quench-flow method but there was an important difference; instead of a small transient P_i burst, there appeared to be a transient lag phase of free P_i . This is confirmed below.

We then set out to confirm that the initial short and rapid myofibrillar ATPase, k^F , represents a true steady-state phase. This made it necessary to separate k^F from the transient kinetics.

Calcium-activated myofibrils: transient kinetics of formation of total and free P_i

The initial time courses for free P_i and total P_i (i.e., the $\text{M} \cdot \text{ADP} \cdot \text{P}_i$ state with or without actin (Scheme 1) plus

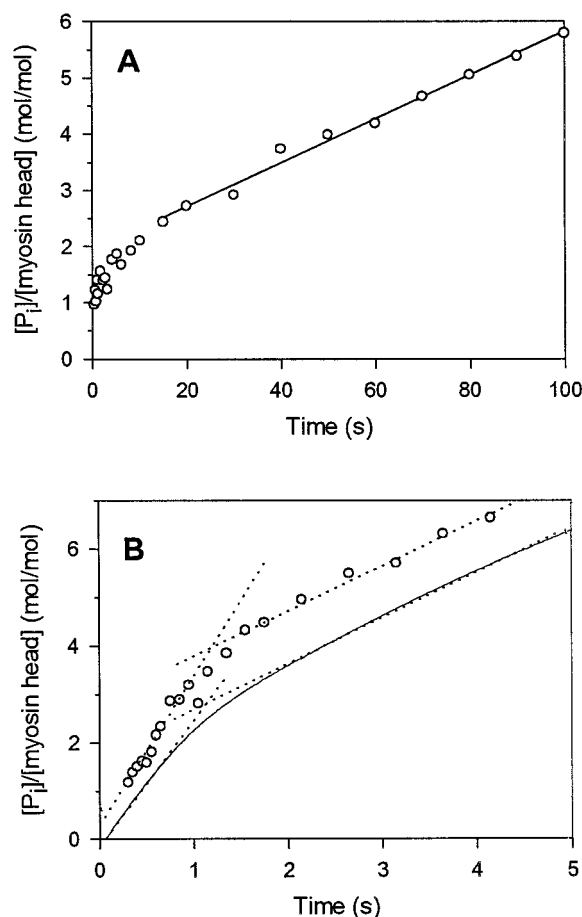


FIGURE 1 Time courses for the ATPases of relaxed (*A*) and Ca^{2+} -activated (*B*) frog tibialis myofibrils at 4°C. (*A*) The reaction mixtures (60 μM [$\gamma\text{-}^{32}\text{P}$]ATP plus 5 μM myosin heads) were quenched in acid at the times shown, and the $^{32}\text{P}_i$ was determined. (*B*) Total P_i formation was followed by quench flow (○; reaction mixtures as in *A*) and free P_i by fluorescence stopped flow (—; reaction mixture, 50 μM ATP plus 0.25 μM myosin heads). In both experiments, the dashed lines represent k^F and k^S .

free P_i) are shown in Fig. 2. These experiments were carried out on myofibrils from mixed fast leg muscle fibers of the frog. For technical reasons, the concentration of ATP was low ($30 \mu\text{M}$).

In the total P_i experiment (quench flow), the time course consisted of a P_i burst phase (amplitude, $0.24 \pm 0.09 \text{ mol } P_i/\text{mol myosin heads}$; kinetics, $14 \pm 7 \text{ s}^{-1}$) followed by a steady-state rate of $2.1 \pm 0.1 \text{ s}^{-1}$.

In the free P_i experiment (PBP, stopped flow) the time course consisted of a transient lag phase (negative burst of $0.12 \pm 0.01 \text{ mol } P_i/\text{mol myosin heads}$; kinetics, $22 \pm 1 \text{ s}^{-1}$) followed by a steady-state rate of $2.14 \pm 0.01 \text{ s}^{-1}$.

There are three noteworthy features of these experiments. First, they show that the P_i burst obtained by quench flow is due to protein-bound P_i ($(A)M \cdot ADP \cdot P_i$, Scheme 1). Thus, the lag in free P_i production corresponded well to the burst kinetics in the formation of total P_i , i.e., the buildup of $(A)M \cdot ADP \cdot P_i$. Second, the steady-state rates agree well with each other and with the estimates for k^F obtained in the longer time range (e.g., Fig. 1). This is important because, in the transient kinetics experiments, the steady-state rates were obtained as early as possible, just after the transient phases, i.e., before any significant shortening had occurred (Figs. 2 and 6). Third, consider the kinetics of the P_i burst in the quench-flow experiments, carried out at $30 \mu\text{M}$ ATP. These are directed by the ATP binding and cleavage kinetics. As the kinetics of the burst was $14 \pm 7 \text{ s}^{-1}$, the second-order binding constant for ATP is $\geq 0.5 \pm 0.2 \mu\text{M}^{-1} \text{ s}^{-1}$.

Because of the high concentrations of myofibrils needed, it was difficult to measure directly the kinetics of the ATP cleavage step by the quench-flow method. However, by

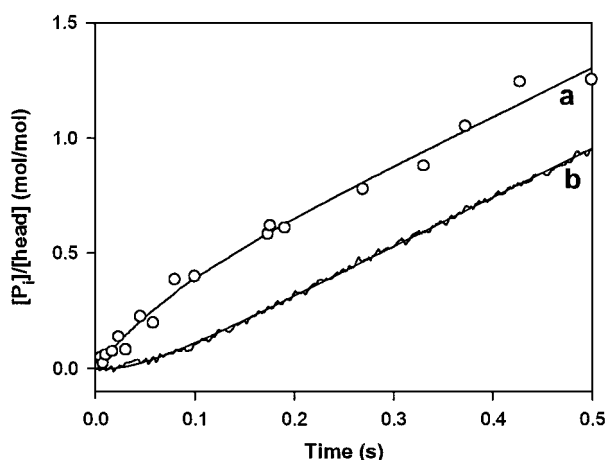


FIGURE 2 Initial time courses of total (a) and free (b) P_i with Ca^{2+} -activated myofibrils from mixed fast frog muscles at 4°C . (a) Quench flow. The reaction mixtures were $30 \mu\text{M}$ $[\gamma\text{-}^{32}\text{P}]\text{ATP}$ plus $3 \mu\text{M}$ myosin heads. (b) Fluorescence stopped flow; $30 \mu\text{M}$ ATP plus $0.25 \mu\text{M}$ heads. In a, the data fit to a transient burst phase (amplitude, $0.24 \pm 0.09 \text{ mol } P_i/\text{mol myosin head}$; kinetics, $14 \pm 7 \text{ s}^{-1}$) and a steady-state rate of $2.1 \pm 0.1 \text{ s}^{-1}$. (b) The data fit to a transient lag phase (negative amplitude, $0.12 \pm 0.1 \text{ mol } P_i/\text{mol myosin head}$; kinetics, $22 \pm 1 \text{ s}^{-1}$) and a steady-state rate of $2.14 \pm 0.01 \text{ s}^{-1}$.

exploiting the kinetics of the transient lag phase in the PBP experiments, we obtained an estimate for these kinetics and also the second-order constant for ATP binding.

The dependence of the lag-phase kinetics on the ATP concentration is illustrated in Fig. 3. We interpret the non-linearity by a change in rate-limiting step; at low ATP, k_{obs} is directed by the ATP binding ($0.8 \mu\text{M}^{-1} \text{ s}^{-1}$) and at high ATP by cleavage kinetics ($50\text{--}60 \text{ s}^{-1}$). With the aid of these transient kinetic data, we now return to the steady-state parameters k^F and k^S .

Myofibrillar steady-state parameters k^F and k^S

How we obtained estimates

At $30 \mu\text{M}$ ATP, k^F was obtained directly from the steady-state rates immediately following the transient phases in initial total and free P_i time courses (Fig. 2). The rates obtained by the two methods agreed well.

For our estimates of k^S , we refer to Fig. 1 B. In the quench-flow experiment, the curvature toward the end of the time course can be explained by depletion of the ATP. In the PBP experiment, there was a distinct curvature at times greater than 5 s (not shown), which could be due to the presence of the PBP mop system (Lionne et al., 1995). To estimate k^S , for example at $60 \mu\text{M}$ ATP, we assumed that P_i production in the 2.5–4 s time range was linear. At higher ATP concentrations, the linear time range was earlier.

Effects of the concentration of ATP on the myofibrillar ATPase parameters

The dependences of k^F and k^S on the ATP concentration are shown in Fig. 4. In each dependence, a hyperbola fits the data reasonably well.

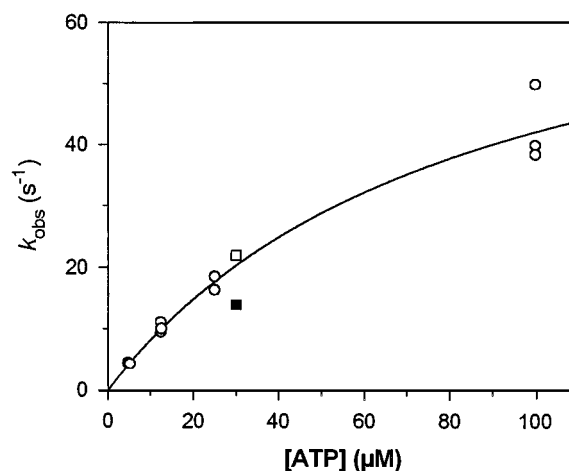


FIGURE 3 Dependence of the kinetics of the transient lag phase in fluorescence stopped-flow experiments (free P_i formation) on the ATP concentration with Ca^{2+} -activated myofibrils at 4°C . The experiments were as in Fig. 2 with the myofibrillar concentration constant at $0.25 \mu\text{M}$ (myosin heads). The data were obtained with myofibrils from tibialis (○) and mixed fast muscle fibers (□). ■, kinetics of the total P_i burst in Fig. 2.

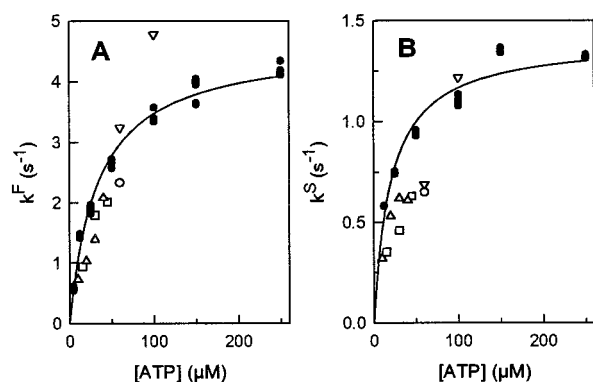


FIGURE 4 Dependences of the ATPase parameters of Ca^{2+} -activated myofibrils (tibialis) on the ATP concentration at 4°C. ●, data from fluorescence stopped-flow experiments (PBP method); △, ○, and □, quench-flow data with different symbols indicating different preparations. For details of how k^F and k^S were estimated, see Fig. 1 and the text. For each parameter, the PBP data were fitted to hyperbolas, and the kinetic constants obtained are in Table 1.

Only the data from the PBP experiments were used to obtain the maximal and K_M values, but as can be seen, the quench-flow experiments gave k^F values in reasonable agreement with the PBP data.

The maximal and K_M values for each parameter are given in Table 1 where they are compared with those obtained with rabbit psoas myofibrils.

Temperature dependences of k^F and k^S

The two temperature dependences are illustrated in Fig. 5. The ΔH^\ddagger enthalpy of activation values obtained are similar to those obtained with rabbit psoas myofibrils (Table 1).

Myofibrillar shortening velocities by the quench-flow method

The myofibrillar (tibialis) shortening velocities were studied at two concentrations of ATP (60 μM and 1 mM ATP), and

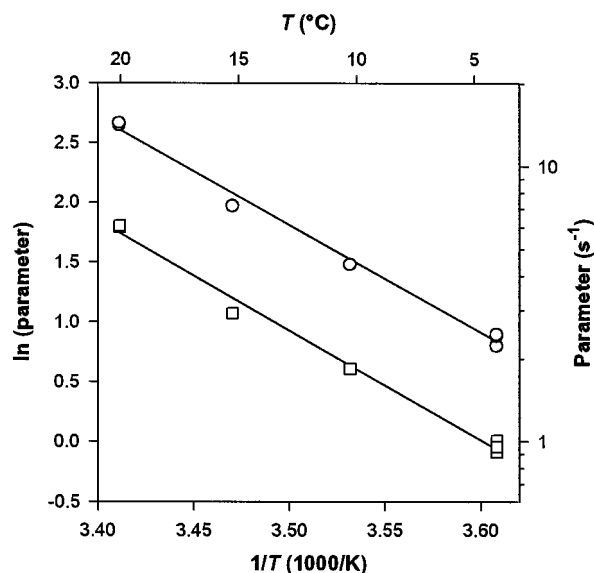


FIGURE 5 Arrhenius plots of the myofibrillar ATPase parameters. The parameters were obtained from fluorescence stopped-flow experiments (e.g., Fig. 1) with 150 μM ATP and 0.25 μM myosin heads. ○, k^F ; □, k^S . The ΔH^\ddagger values obtained are in Table 1.

the time courses are illustrated in Fig. 6, which also includes the ATPase time course at 50 μM ATP. There are several noteworthy features of these experiments.

In the shortening experiment at 60 μM ATP (Fig. 6 A), there was a lag phase of ~ 150 ms, followed by a reasonably linear rapid shortening process with a rate of 0.62 ($\mu\text{m}/\text{h.s.}$) s^{-1} and then a progressive deceleration to 0.04 ($\mu\text{m}/\text{h.s.}$) s^{-1} . The two shortening rates extrapolated to a break at ~ 1 s. In the experiment at 1 mM ATP, a lag phase was not discerned. At this ATP concentration, the initial shortening rate was rapid at 2 ($\mu\text{m}/\text{h.s.}$) s^{-1} , and there was a change to 0.13 ($\mu\text{m}/\text{h.s.}$) s^{-1} with the break at 0.22 s. From the rapid shortening processes in the two experiments, we can roughly estimate that, at saturation in ATP, the maximal shortening velocity is ~ 2.4 ($\mu\text{m}/\text{h.s.}$) s^{-1} with a K_m for ATP of ~ 200 μM . These data agree well with the shortening parameters obtained from mechanical measurements (slack test) performed with single myofibrils from frog tibialis (Table 2). It is noteworthy that the breaks in the shortening and ATPase rates appear to occur at the same time.

In both shortening experiments, the mean initial sarcomere lengths were 2.25 μm , and rapid shortening occurred approximately linearly over a distance of 0.5–0.6 μm . Over this shortening distance, the overall sarcomere structure of the myofibril was retained (as seen under the microscope). As shortening proceeded, the shortening rate decelerated and myofibrils of abnormally short sarcomere lengths appeared (< 1.3 μm). At very long reaction times (e.g., 4 s at 1 mM ATP), amorphous aggregates were the dominant features. Aggregates were also detected during the intermediate, slow shortening process.

TABLE 1 ATPase parameters for myofibrils from frog and rabbit fast muscle fibers at 4°C

Parameter	Myofibrils from	
	Frog tibialis	Rabbit psoas*
Activated (with Ca^{2+})		
$k^F:k^F_{\text{max}}$ (s^{-1})	4.6 ± 0.1	1.7 ± 0.1
K_m (μM)	33 ± 2	9 ± 2
ΔH^\ddagger (kJ/mol)	74 ± 3	68 ± 2
$k^S:k^S_{\text{max}}$ (s^{-1})	1.4 ± 0.05	0.33 ± 0.05
K_m (μM)	20 ± 1	5.3 ± 0.8
ΔH^\ddagger (kJ/mol)	76 ± 3	67 ± 2
Relaxed (without Ca^{2+})		
k_{ss} (s^{-1})	0.04 ± 0.01	0.019 ± 0.04

For definitions of parameters and experimental conditions, see text and Fig. 1.

*From Lionne et al. (1996) and Herrmann et al. (1992).

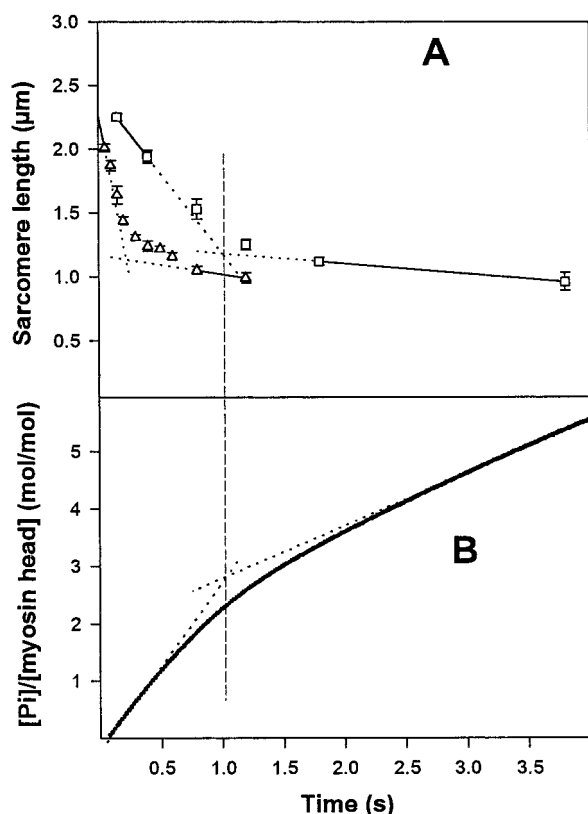


FIGURE 6 (A) Time courses for myofibrillar shortening at two ATP concentrations. Reaction mixtures of 60 μM (\square) or 1 mM (\triangle) ATP plus 1 μM myofibrils (as myosin heads) were quenched at pH 3.5 at the times shown, and the sarcomere lengths were measured under the microscope. In each experiment, the data were fitted to two shortening rates (fast and slow) with a break at time t , respectively: for 60 μM ATP, 0.62 ($\mu\text{m}/\text{h.s.}$) s^{-1} , 0.04 ($\mu\text{m}/\text{h.s.}$) s^{-1} , and 1.0 s; for 1 mM ATP, 2 ($\mu\text{m}/\text{h.s.}$) s^{-1} , 0.13 ($\mu\text{m}/\text{h.s.}$) s^{-1} , and 0.22 s. (B) Time course of the myofibrillar ATPase at 50 μM ATP (PBP method, Fig. 1 B), to show the correspondence of the breaks in the shortening experiment (\square) and ATPase rates. In all experiments, the initial sarcomere lengths were 2.25 μm and the temperature was 4°C.

DISCUSSION

Analysis of the myofibrillar ATPase and shortening time courses

In this study we measured the ATPase activity of unheld, Ca^{2+} -activated myofibrils by two methods: chemical sampling (in which total P_i is determined) and by the PBP technique (specific for free P_i). We interpret our ATPase progress curves by three phases:

Initial P_i burst

The initial P_i burst is due to protein-bound P_i (as (A)M \cdot ADP \cdot P_i , see below).

Fast ATPase, k^F

The fast ATPase is the ATPase of myofibrils that are shortening rapidly, first, because shortening and k^F occurred in the same time range (Fig. 6 B) and, second, because the deceleration of the shortening and ATPase rates occurred at the same time. Furthermore, with rabbit psoas myofibrils that were prevented from shortening by chemical cross-linking, there was only one, fast, ATPase activity (Herrmann et al., 1993).

Slow ATPase, k^S

In the slow ATPase time range, myofibrils have sarcomere lengths shorter than the length of the thick filaments ($<1.65 \mu\text{m}$). Nevertheless, these myofibrils continue to shorten slowly, leading eventually to a loss of structure.

We also measured myofibrillar shortening velocities at high and low ATP concentrations by quench flow and by examining sarcomere lengths under the microscope (Fig. 6). In the two experiments, the shortening velocity appears to be constant when the sarcomere lengths shortened from 2.25 to $\sim 1.7 \mu\text{m}$ (Fig. 6). This is in agreement with Edman (1979) who showed that, with frog muscle fibers (semiten-dinosus muscle from *Rana temporaria*), V_0 was constant when the sarcomere lengths were between 1.65 and 2.7 μm . The deceleration in shortening at sarcomere lengths $<1.7 \mu\text{m}$, observed both by Edman (1979) and here, is presumably a result of an increase in internal resistance, as at 1.7 μm , the sarcomeres are near the thick filament length.

The reason the deceleration of the ATPase rate parallels that of the shortening velocity is not completely clear. At short sarcomere lengths, there could be an increase in the internal load, but it is difficult to predict the effect of this upon the myofibrillar ATPase rate. It could be that at short sarcomere lengths there is a reduction in the effective overlap and as shortening proceeds further, the myofibrillar lattice structure is impaired. Together, these effects would reduce the myosin head-actin interaction and therefore the overall ATPase activity.

The lag phase in the shortening experiment at 60 μM ATP (Fig. 6) implies that during the first 150 ms there is little shortening. Because of its sensitivity to the ATP concentration (at 1 mM ATP, a lag could not be detected), the lag could be connected with the ATP binding. However, these binding kinetics ($\sim 30 \text{ s}^{-1}$ at 60 μM) are too fast for a lag of 150 ms. Another explanation is that the lag represents the time it takes for all of the heads to become detached. Thus, with myofibrils from rabbit psoas, shortening is prevented when as few as 8% of the heads are attached (Herrmann et al., 1993).

TABLE 2 Frog myofibrillar (tibialis) shortening rates

Method	Shortening parameters	
	V_0^{max} ($\mu\text{m}/\text{h.s.}$) s^{-1}	K_m (μM)
Shortening experiment (Fig. 6), 4°C	~ 2.4	~ 200
Slack test,* 5–7°C	3.6 ± 0.2	190 ± 40

*S. Nencini, N. Piroddi, C. Poggesi, and C. Tesi, unpublished results.

Myofibrillar shortening velocities by quench flow: comparison with muscle fiber work

The myofibrillar shortening parameters (V_0^{\max} and K_m for ATP) obtained by quench flow agree well with the mechanical measurements (Table 2). This agreement is important; it suggests that, in at least one mechanical property, myofibrils behave similarly, whether they are freely dispersed in buffer (as here) or investigated individually under more controlled conditions (as in the mechanical experiments).

The estimates for the maximal myofibrillar shortening velocity are in accord with the V_0 ($\mu\text{m/h.s.}$) s^{-1} obtained with anuran muscle fibers at 2–4°C: *R. temporaria*, 2.7 (Edman, 1979) and 2.5 (Ferenczi et al., 1984), and *Xenopus laevis*, 1.9 (Stienen et al., 1988). However, myofibrils have a smaller K_m for ATP: 200 μM compared with 470 μM for fibers from *R. temporaria* (Ferenczi et al., 1984) and 540 μM with fibers from *X. laevis* (Stienen et al., 1988).

Comparison of myofibrillar and fiber ATPases

Whereas there are few direct data on the ATPase activities of anuran fast muscle preparations, there is a large body of information on the energetics of muscle contraction in the frog. ATP hydrolysis by frog fast skeletal muscle at 0°C has been estimated in energy balance studies from both myothermal and biochemical measurements (for reviews see Kushmerick, 1983; Homsher, 1987), and we must see whether our data fit in with these studies. Furthermore, we must consider the very recent work of He et al. (1997) in which high ATPase rates are reported for skinned muscle fibers from the frog and rabbit.

Muscle energetics and myofibrillar ATPases

Relaxing conditions

We estimate a rate of 0.04 s^{-1} (at 4°C) for the ATPase of frog myofibrils, which is similar to the 0.05 s^{-1} found by Ferenczi et al. (1978a). These values are in reasonable agreement with the ATPase rates determined from the aerobic metabolism (0.024 s^{-1} ; Kushmerick and Paul, 1976) or high-energy phosphate metabolism (0.035 s^{-1} ; Levy et al., 1976) of whole frog sartorius muscle at 0°C. These frog ATPases are considerably higher than that of rabbit psoas myofibrils (Table 1).

Activating conditions

With fully activated myofibrils at 4°C, the ATPase rate was 4.6 s^{-1} (k^F , Table 1). Ferenczi et al. (1978a) obtained a low ATPase rate of 0.44 s^{-1} with a similar preparation, at 0–2°C. However, their time course was on the minutes time scale, i.e., well after the initial shortening process had occurred, and their rate probably refers to overcontracted myofibrils.

It is noteworthy that the ATPase activity of shortening myofibrils from a cold-blooded animal (frog) is almost three times higher than that from the warm-blooded rabbit (Table 1). This is in agreement with the muscle fiber work of Stephenson et al. (1989) who obtained an isometric ATPase rate of 6.35 s^{-1} with fast muscle fibers from the cane toad (*Bufo marinus*) and 3.8 s^{-1} for the rat (*Rattus norvegicus*) at 20–25°C.

A comparison of the maximal ATPase activity of unheld myofibrils with that of actively contracting whole-muscle preparations is difficult because, with the latter, ATP hydrolysis depends strongly on the mechanical condition of contraction (Woledge et al., 1985, and references cited therein). Recently, Chaen et al. (1997) showed that, with held myofibrils and a fluorescent analogue of ATP, the rate of substrate cleavage depended on the shortening velocity. This dependence is as expected as the rate of enthalpy liberation by isotonically contracting muscle (largely a reflection of the rate of enthalpy liberation upon ATP hydrolysis) increases with the shortening velocity in a characteristic way (Hill, 1938). Consequently, the ATPase activity of unheld myofibrils is comparable only with that of muscle preparations shortening at near V_0 . With frog skeletal muscle, this activity has been obtained only from muscle energetics.

In energy balance studies, direct measurements of the ATPase activity of isotonically contracting frog fast muscles showed that, at velocities approaching V_0 , the amount of ATP hydrolyzed was much lower than that expected from the rate of enthalpy liberation; indeed, it was not too different from that found in isometric conditions (1–2 s^{-1} ; Kushmerick and Davies, 1969; Homsher et al., 1981, 1984). This low ATP utilization during rapid shortening was explained by Homsher et al. (1981) by a time lag between the liberation of energy and ATP hydrolysis during rapid shortening and the balance recovering during the isometric post-shortening phase.

The value we estimated for the ATPase rate of frog myofibrils, 4.6 s^{-1} , was obtained with unheld myofibrils shortening at zero external load. This value is higher than the isometric ATPase rate estimated in frog muscle preparations although it fits reasonably well with the ATPase rate expected from the rate of the enthalpy change measured during rapid shortening (Hill, 1938; Linari and Woledge, 1995). Our results therefore suggest that, at least under our conditions with unheld myofibrils in solution, ATP hydrolysis matches the energy liberation process with little delay.

Do the ATPase kinetics in isometric fibers and unheld myofibrils agree?

He et al. (1997) reported a very high ATPase activity for isometrically held, Ca^{2+} -activated muscle fibers from frog (semitendinosus from *R. temporaria*). Contraction was triggered by the photolysis of caged ATP and free P_i production followed by the PBP method under conditions similar to

those used here. The PBP time course was biphasic: during the first two turnovers (up to 0.2 s), a rapid ATPase activity of 16.4 s^{-1} followed by a reduction to 2.8 s^{-1} . In agreement with our work, there was little evidence for a transient burst of free P_i .

With the rabbit psoas, too, the initial fiber ATPase rate was higher than that of myofibrils. Thus, at 20°C , they were 40.6 s^{-1} and 8.3 s^{-1} , respectively (He et al., 1997; Herrmann et al., 1994). Chemically cross-linked myofibrils (which may mimic the isometric condition) have an ATPase rate of 3.5 s^{-1} (Herrmann et al., 1993). As at 20°C , the fiber ATPase rate is close to that of acto-S1, He et al. (1997) propose that initially all the cross-bridges are attached to the thin filament and therefore function simultaneously as maximally actin-activated ATPase sites. However, at 5°C , the fiber ATPase rate (He et al., 1997) is almost an order of magnitude greater than that of rabbit acto-S1 ATPase (Herrmann et al., 1994): 9 and 1.3 s^{-1} , respectively. The myofibrillar ATPase rate (k^F) was 1.9 s^{-1} (Herrmann et al., 1994). The low acto-S1 ATPase at 5°C is explained by its high ΔH^\ddagger of 109 kJ/mol (Herrmann et al., 1994) whereas the ΔH^\ddagger values of the fiber and myofibrillar (k^F) ATPases are similar at 70 kJ/mol (He et al., 1997) and 62 kJ/mol (Herrmann et al., 1994), respectively.

How do we reconcile these differences between the fiber and myofibrillar ATPases? We consider six potential causes.

First, the measurements were made under different mechanical conditions; i.e., it could be that the P_i -release kinetics with isometric fibers are just faster than with unheld myofibrils. However, the ATPase rate of chemically cross-linked rabbit myofibrils was lower than with un-cross-linked myofibrils (see above).

Second, He et al. (1997) proposed that, in the previous fiber measurements, the initial, rapid ATPase was missed because the measurements were begun at least 1 s after the initiation of the contraction. This proposal does not explain the lower myofibrillar ATPase rate ($k^F = 4.6 \text{ s}^{-1}$) we measured in unheld myofibrils, also by the PBP method. Our measurements were made immediately after the P_i transients (lag phase in the PBP time course, burst phase in the quench-flow time course, e.g., Fig. 2), and it is unlikely that we missed a rapid ATPase activity in our experiments.

Third, the differences between the two ATPases could be because a higher ATP concentration was used in the fiber measurements, 1 mM rather than $250 \mu\text{M}$ or less with myofibrils. Thus, the differences could be related to different rates of diffusion of ATP in the two materials. In fact, substrate diffusion does not appear to be a problem with myofibrils. With rabbit psoas myofibrils, ATP diffuses rapidly to the myosin heads, at least on the time scale of the measurements, and the ATPase sites behave as though they were in solution, as in myosin or actomyosin (Sleep, 1981; Herrmann et al., 1992, and references cited therein). In particular, in ATP chase experiments (in which ATP binding kinetics are measured specifically), lag transient phases were absent (reaction times, 5 ms to several seconds;

Houadjeto et al., 1992). Such experiments would be expected to be highly sensitive to diffusion. ATP chase experiments also provided estimates for the ATPase site concentrations in myofibrils (these estimates were in good agreement with the myosin head measurements) and the second-order binding constant for ATP (which was close to those found with myosin and actomyosin). Furthermore, with frog myofibrils, there was little evidence for a lag phase in the P_i burst transient (Fig. 2 *a*).

Fourth, an explanation for the lower myofibrillar ATPase is that not all of the heads are fully activated in this preparation, even at saturating Ca^{2+} concentrations. This would explain the results, at least at 20°C but not at 5°C (see above). Furthermore, it would imply that in myofibrils only approximately one-third of the heads are activated. This seems unlikely because, first, the active and passive forces in myofibrils are similar to those in fibers (Colomo et al., 1997, and references cited therein) and, second, myofibrillar and fiber shortening velocities are in agreement (S. Nencini, N. Piroddi, C. Poggesi, and C. Tesi, unpublished results; see Table 2).

Fifth, it could be that in fibers the myofibrils are organized so they contract cooperatively, which would result in a higher ATPase rate than with the dispersed myofibrils. However, this would not explain the mechanical similarities between fibers and myofibrils.

Finally, there is the notion of active site concentrations in organized systems, which, of course, are needed to obtain k_{cat} . With myofibrils, as discussed above, these concentrations appear to be readily obtained. With fibers, the situation may be more difficult, as discussed by He et al. (1997). However, the discrepancy on the ATPase measurements seems too large to be explained by possible errors in this concentration.

Identifying the predominant intermediates on frog myofibrillar ATPase

The intermediates on the myosin ATPase pathway (Scheme 1) interact in different ways with the thin filament, and it is this interaction that is responsible for the contractile process. Therefore, to fully understand muscle contraction we must identify the predominant intermediates and determine their rates of interconversion. The P_i burst method is an important method for identifying ATPase intermediates (Lymn and Taylor, 1970). In this, reaction mixtures are quenched in acid and the P_i determined; this is total P_i as it includes enzyme-bound $((\text{A})\text{M} \cdot \text{ADP} \cdot \text{P}_i)$ as well as free P_i .

In Fig. 2 we show that there is a significant P_i burst with frog myofibrils. As the ATP concentration used in the experiment was lower than the K_m for ATP ($30 \mu\text{M}$ compared with $33 \mu\text{M}$) the amplitude obtained ($0.24 \mu\text{mol P}_i$ per mol myosin head) is a minimum value. This P_i burst shows that $(\text{A})\text{M} \cdot \text{ADP} \cdot \text{P}_i$ and/or $\text{AM} \cdot \text{ADP}$ are important intermediates on the myofibrillar reaction pathway. To deter-

mine which, we studied free P_i production by the PBP method, and as can be seen in Fig. 2, there was a large transient lag phase in the progress curve. This is strong evidence that P_i release is the rate-limiting step of the ATPase cycle, i.e., that the P_i burst in the quench-flow experiment is due to the $(A)M \cdot ADP \cdot P_i$ states and that the concentration of $AM \cdot ADP$ is low.

It appears, therefore, that with Ca^{2+} -activated frog, as with rabbit psoas myofibrils (Lionne et al., 1995), the $(A)M \cdot ADP \cdot P_i$ states predominate in the steady state. It has been proposed that both $AM \cdot ADP \cdot P_i$ and $AM \cdot ADP$ contribute to the force-generating state (Dantzig et al., 1992; He et al., 1997, and references cited therein). Should the $AM \cdot ADP$ state be the only relevant force-generating state this would suggest the presence of only a few force-generating cross-bridges during rapid shortening.

Relation between movement and ATP hydrolysis

Two parameters are used to relate the distance moved by a myosin head along an actin filament during hydrolysis of one ATP molecule: sliding distance and power stroke. Here these refer to the situation of unloaded myofibrillar shortening. The sliding distance is the physical distance traveled by a cross-bridge along the thin filament per molecule of ATP hydrolyzed. This distance can be estimated by dividing V_o by the ATPase rate during the shortening (both at saturating ATP), i.e., $2.4 (\mu\text{m/h.s})\text{s}^{-1}/4.6 \text{ s}^{-1} = 520 \text{ nm}$ (Tables 1 and 2).

The power stroke can be defined as the distance moved by each attached head during the hydrolysis of one ATP molecule by that head. This distance is determined largely by the length of the myosin head and by the amplitude of its conformation change and is assumed to be 5–10 nm (reviewed in Cooke, 1997). From chemical kinetic experiments (e.g., Fig. 1), most of the myosin heads participate in ATP hydrolysis.

The large difference of the two parameters suggests strongly that, at any one time, only 1–2% of the heads are attached and actually producing rapid sliding. This is in reasonable agreement with the duty ratio as discussed by Cooke (1997). At any one time, the few heads that are attached undergo the 5- to 10-nm movement of the power stroke, whereas the detached majority of heads move 520 nm (with respect to the thin filament) as passengers (e.g., Irving, 1991; Cooke et al., 1994).

From the biochemical cycle (Scheme 1), most of the heads have bound $ADP \cdot P_i$ and, as few are attached, the predominant intermediate is $M \cdot ADP \cdot P_i$. Therefore, whereas, chemically, P_i release is rate limiting, this process is itself limited by reattachment ($M \cdot ADP \cdot P_i$ to $AM \cdot ADP \cdot P_i$). It follows that the concentration of $AM \cdot ADP \cdot P_i$ is low because the actual P_i release step is faster than the formation of $AM \cdot ADP \cdot P_i$. In this respect, it is similar to the situation with acto-S1 from rabbit fast muscle, but in that case, the ATP cleavage step is rate limiting (Rosenfeld and Taylor, 1984; Biosca et al., 1985).

Which step (or steps) in the ATPase cycle (Scheme 1) is connected with V_o ? At low ATP concentrations, it is likely that V_o is limited by the rate of ATP binding (e.g., Ferenczi et al., 1984; Goldman, 1987). As the ATP concentration is increased, V_o increases until a saturation plateau is reached, and so presumably another step limits V_o . From the discussion above, this step is likely to involve an attached state; once a cross-bridge is attached it must go through its power stroke as quickly as possible and detach, as otherwise it may cause a negative strain on the other heads going through their power strokes. In this simple model, the rate limiting these processes involving attached states will be V_o divided by the power stroke, $250\text{--}500 \text{ s}^{-1}$, i.e., approximately two orders of magnitude greater than k_F^{max} (4.6 s^{-1}). This difference in V_o and k_F^{max} would explain the different K_m values for the two processes: ~ 200 and $33 \mu\text{M}$, respectively (Tables 1 and 2).

Based on a comparison of different muscle types, Siemankowski et al. (1985) proposed that, at high ATP concentrations, shortening is limited by the ADP release kinetics. This proposal is consistent with the low duty ratio of the shortening myofibrils, as the concentration of free P_i and, therefore, the proposed key intermediate $AM \cdot ADP$ are very low (Fig. 2). However, more recently, White et al. (1997) proposed that an earlier step on the myosin head ATPase pathway limits V_o when a variety of nucleotide analogs are used to measure fiber shortening velocity (Pate et al., 1993) and acto-S1 ATPase (White et al., 1993, 1997). The kinetics of the P_i release steps do not vary much with substrate and so are unlikely to be responsible for the differences observed in the shortening velocities. Because the kinetics of the cleavage step is the main one that varies significantly with nucleotide, White et al. (1997) proposed that, when the rate of this step is reduced by use of nucleotide analogs, it becomes involved in limiting V_o .

In conclusion, with ATP as the substrate, there may be at least two steps in balance that control V_o . To allow shortening without significant impediment from negatively strained cross-bridges, the attached states go through the power stroke at a rate balanced by the formation of passenger states (mainly $M \cdot ADP \cdot P_i$). Increasing the rate of either one process may not produce any significant advantage.

This work was supported by the European Union, the Medical Research Council (UK), Telethon-Italy, Università degli Studi di Firenze, and NATO. R. Stehle was supported by an INSERM postdoctoral fellowship and C. Lionne is grateful to the Association Française contre les Myopathies for financial support.

REFERENCES

- Barman, T. and F. Travers. 1985. The rapid flow-quench method in the study of fast reactions in biochemistry: extension to subzero temperatures. *Methods Biochem. Anal.* 31:1–59.
- Bartoo, M. L., V. I. Popov, L. A. Fearn, and G. H. Pollack. 1993. Active tension generation in isolated skeletal myofibrils. *J. Muscle Res. Cell Motil.* 14:498–510.

- Biosca, J. A., F. Travers, T. Barman, R. Bertrand, E. Audemard, and R. Kassab. 1985. Transient kinetics of ATP hydrolysis by covalently cross-linked actomyosin complex in water and 40% ethylene glycol by the rapid flow quench method. *Biochemistry*. 24:3814–3820.
- Brenner, B. 1980. Effect of free sarcoplasmic Ca^{2+} concentration on maximum unloaded shortening velocity: measurements on single glycerinated rabbit psoas muscle fibres. *J. Muscle Res. Cell. Motil.* 1:409–428.
- Brune, M., J. L. Hunter, J. E. T. Corrie, and M. R. Webb. 1994. Direct, real-time measurement of rapid inorganic phosphate release using a novel fluorescent probe and its application to actomyosin subfragment-1 ATPase. *Biochemistry*. 33:8262–8271.
- Cecchi, G., F. Colomo, and V. Lombardi. 1978. Force-velocity relation in normal and nitrate-treated frog single muscle fibres during rise of tension in an isometric tetanus. *J. Physiol.* 285:257–273.
- Chaen, S., I. Shirakawa, C. R. Bagshaw, and H. Sugi. 1997. Measurement of nucleotide release kinetics in single skeletal muscle myofibrils during isometric and isovelocity contraction using fluorescence microscopy. *Biophys. J.* 73:2033–2042.
- Colomo, F., N. Piroddi, C. Poggesi, G. Kronnie, and C. Tesi. 1997. Active and passive forces of isolated myofibrils from cardiac and fast skeletal muscle of the frog. *J. Physiol.* 500:535–548.
- Cooke, R. 1997. Actomyosin interactions in striated muscle. *Physiol. Rev.* 77:671–697.
- Cooke, R., H. White, and E. Pate. 1994. A model of the release of myosin heads from actin in rapidly contracting muscle fibers. *Biophys. J.* 66:778–788.
- Dantzig, J. A., Y. E. Goldman, N. C. Millar, J. Lactis, and E. Homsher. 1992. Reversal of the cross-bridge force-generating transition by photogeneration of phosphate in rabbit psoas muscle fibres. *J. Physiol.* 451:247–278.
- Edman, K. A. P. 1979. The velocity of unloaded shortening and its relation to sarcomere length and isometric force in vertebrate muscle fibres. *J. Physiol.* 291:143–159.
- Ferenczi, M. A., E. Homsher, D. R. Trentham, and A. G. Weeds. 1978a. Preparation and characterization of frog muscle myosin subfragment 1 and actin. *Biochem. J.* 171:155–163.
- Ferenczi, M. A., E. Homsher, R. M. Simmons, and D. R. Trentham. 1978b. Reaction mechanism of the magnesium ion-dependent adenosine triphosphatase of frog muscle myosin and subfragment 1. *Biochem. J.* 171:165–175.
- Ferenczi, M. A., Y. E. Goldman, and R. M. Simmons. 1984. The dependence of force and shortening velocity on substrate concentration in skinned muscle fibres from *Rana temporaria*. *J. Physiol.* 350:519–543.
- Ford, L. E., A. F. Huxley, and R. E. Simmons. 1977. Tension responses to sudden length changes in stimulated frog muscle fibres near slack length. *J. Physiol.* 269:441–515.
- Ford, L. E., K. Nakagawa, J. Desper, and C. Y. Seow. 1991. Effect of osmotic compression on the force velocity properties of glycerinated skeletal muscle cells. *J. Gen. Physiol.* 97:73–86.
- Friedman, A., and Y. E. Goldman. 1996. Mechanical characterization of skeletal muscle myofibrils. *Biophys. J.* 71:2774–2785.
- Geeves, M. A. 1991. The dynamics of actin and myosin association and the cross-bridge model of muscle contraction. *Biochem. J.* 274:1–14.
- Goldman, Y. E. 1987. Kinetics of the actomyosin ATPase in muscle fibres. *Annu. Rev. Physiol.* 49:637–654.
- Gordon, A. M., A. F. Huxley, and F. J. Julian. 1966. The variation in isometric tension with sarcomere length in vertebrate muscle fibres. *J. Physiol.* 184:170–192.
- He, Z.-H., R. K. Chillingworth, M. Brune, J. E. T. Corrie, D. R. Trentham, M. R. Webb, and M. R. Ferenczi. 1997. ATPase kinetics on activation of rabbit and frog permeabilized isometric muscle fibres: a real time phosphate assay. *J. Physiol.* 501:125–148.
- Herrmann, C., M. Houadjetto, F. Travers, and T. Barman. 1992. Early steps of the Mg^{2+} -ATPase of relaxed myofibrils: a comparison with Ca^{2+} -activated myofibrils and myosin subfragment 1. *Biochemistry*. 31:8036–8042.
- Herrmann, C., J. Sleep, P. Chaussepied, F. Travers, and T. Barman. 1993. A structural and kinetic study on myofibrils prevented from shortening by chemical cross-linking. *Biochemistry*. 32:7255–7263.
- Herrmann, C., C. Lionne, F. Travers, and T. Barman. 1994. Correlation of actoS1, myofibrillar and muscle fibre ATPases. *Biochemistry*. 33:4148–4154.
- Hill, A. V. 1938. The heat of shortening and the dynamic constants of muscle. *Proc. R. Soc. London Ser. B.* 126:136–195.
- Homsher, E. 1987. Muscle enthalpy production and its relationship to actomyosin ATPase. *Annu. Rev. Physiol.* 49:673–690.
- Homsher, E., M. Irving, and A. Wallner. 1981. High-energy phosphate metabolism and energy liberation associated with rapid shortening in frog skeletal muscle. *J. Physiol.* 321:423–436.
- Homsher, E., T. Yamada, A. Wallner, and J. Tsai. 1984. Energy balance studies in frog skeletal muscle shortening at half of maximum velocity. *J. Gen. Physiol.* 84:347–360.
- Houadjetto, M., F. Travers, and T. Barman. 1992. Ca^{2+} activated myofibrils: transient kinetics and the titration of active sites. *Biochemistry*. 31:1564–1569.
- Huxley, A. F. 1980. Reflections on Muscle. Liverpool University Press, Liverpool.
- Irving, M. 1991. Biomechanics goes quantum. *Nature*. 352:284–285.
- Knight, P. J., and J. A. Trinick. 1982. Preparation of myofibrils. *Methods Enzymol.* 85B:9–12.
- Kushmerick, M. J., and R. E. Davies. 1969. The chemical energetics of muscle contraction. II. The chemistry, efficiency and power of maximally working sartorius muscle. *Proc. R. Soc. London Ser. B.* 174:315–353.
- Kushmerick, M. J. 1983. Energetics of muscle contraction. In *Handbook of Physiology, Section 10: Skeletal Muscle*. American Physiological Society, Bethesda, MD. 189–237.
- Kushmerick, M. J., and R. J. Paul. 1976. Aerobic recovery metabolism following a single isometric tetanus in frog sartorius at 0°C. *J. Physiol.* 254:693–709.
- Levy, R. N., Y. Umazume, and M. J. Kushmerick. 1976. Ca^{2+} dependence of tension and ADP production in segments of chemically skinned muscle fibers. *Biochim. Biophys. Acta.* 430:325–365.
- Linari, M., and R. C. Woledge. 1995. Comparison of energy output during ramp and staircase shortening in frog muscle fibres. *J. Physiol.* 487:699–710.
- Lionne, C., M. Brune, M. R. Webb, F. Travers, and T. Barman. 1995. Time resolved measurements show that phosphate release is the rate limiting step on myofibrillar ATPases. *FEBS Lett.* 364:59–62.
- Lionne, C., F. Travers, and T. Barman. 1996. Mechanochemical coupling in muscle: attempts to measure simultaneously shortening and ATPase rates in myofibrils. *Biophys. J.* 70:887–895.
- Lymn, R. W., and E. W. Taylor. 1970. Transient state phosphate production in the hydrolysis of nucleoside triphosphates by myosin. *Biochemistry*. 9:2975–2983.
- Ma, Y.-Z., and E. W. Taylor. 1994. Kinetic mechanism of myofibrillar ATPase. *Biophys. J.* 66:1542–1553.
- Pate, E., K. Franks-Skiba, H. White, and R. Cooke. 1993. The use of differing nucleotides to investigate cross-bridge kinetics. *J. Biol. Chem.* 268:10046–10053.
- Pate, E., G. J. Wilson, M. Bhimani, and R. Cooke. 1994. Temperature dependence of the inhibitory effects of orthovanadate on shortening velocity in fast skeletal muscle. *Biophys. J.* 66:1554–1562.
- Reimann, E. M., and R. A. Umfleet. 1978. Selective precipitation of $^{32}\text{P}_i$ onto filter papers. *Biochim. Biophys. Acta.* 523:516–521.
- Rosenfeld, S. S., and E. W. Taylor. 1984. The ATPase mechanism of skeletal and smooth muscle acto-S1. *J. Biol. Chem.* 259:11908–11919.
- Siemankowski, R. F., M. O. Wiseman, and H. D. White. 1985. ADP dissociation from actomyosin subfragment 1 is sufficiently slow to limit the unloaded shortening velocity in vertebrate muscle. *Proc. Natl. Acad. Sci. U.S.A.* 82:658–662.
- Sleep, J. A. 1981. Single turnovers of ATP by myofibrils and actomyosin subfragment 1. *Biochemistry*. 20:5043–5051.
- Stephenson, D. G., A. W. Stewart, and G. J. Wilson. 1989. Dissociation of force from myofibrillar MgATPase and stiffness at short sarcomere lengths in rat and toad skeletal muscle. *J. Physiol.* 410:351–366.

- Stienen, G. J. M., W. J. Van der Laarse, and G. Elzinga. 1988. Dependency of the force-velocity relationships on MgATP in different types of muscle fibers from *Xenopus laevis*. *Biophys. J.* 53:849–855.
- Taylor, E. W. 1979. Mechanism of actomyosin ATPase and the problem of muscle contraction. *CRC Crit. Rev. Biochem.* 6:102–164.
- Trentham, D. R., J. F. Eccleston, and C. R. Bagshaw. 1976. Kinetic analysis of ATPase mechanisms. *Q. Rev. Biophys.* 9:217–281.
- White, H. D., B. Belknap, and W. Jiang. 1993. Kinetics of binding and hydrolysis of a series of nucleoside triphosphates by actomyosin S1. *J. Biol. Chem.* 268:10039–10045.
- White, H. D., B. Belknap, and M. R. Webb. 1997. Kinetics of nucleoside triphosphate cleavage and P_i release steps by associated rabbit skeletal actomyosin, measured using a novel fluorescent probe for P_i . *Biochemistry*. 36:11828–11836.
- Woledge, R. C., N. A. Curtin, and E. Homsher. 1985. *Energetic Aspects of Muscle Contraction*. Academic Press, London.